

Structural, Optical and Electrical Properties of Transparent Conducting Oxide Based on Al Doped ZnO Prepared by Spray Pyrolysis

Abdeslam DOUAYAR, Hassan BIHRI, Ahmed Mzerd,
Azzam, BELAYACHI and ¹Mohammed ABD-LEFDIL

Université Mohammed V-Agdal, Faculté des Sciences, LPM, B.P. 1014, Rabat, Morocco
Tel./fax: +212 (0) 537778973
E-mail: a-lefdil@fsr.ac.ma

Received: 31 December 2012 /Accepted: 10 August 2013 /Published: 26 May 2014

Abstract: Aluminum doped zinc oxide (AZO) thin films were deposited on glass substrates at 350 °C by spray pyrolysis technique. X-ray diffraction patterns show that the undoped and AZO films exhibit the hexagonal wurtzite crystal structure with a preferential orientation along [002] direction. AFM images showed that AZO film with 3 % of Al has a uniform grain sizes with a surface roughness of about 24 nm. All films present a high transmittance in the visible range. Both undoped and AZO films were n-type degenerate semiconductor and the best electrical resistivity value was around $8.0 \cdot 10^{-2} \Omega \cdot \text{cm}$ obtained for 3 % Al content. *Copyright © 2014 IFSA Publishing, S. L.*

Keywords: Al-doped zinc oxide, Sprayed thin films.

1. Introduction

Doped ZnO thin films received extensive attention due to their excellent optical and electrical properties [1-5]. It is widely used in various technological applications, such as in solar cells and flat panel display [6]. It is also used in sensors devices for gases detection, such as NO₂, NH₃ and CO [7, 8].

Different deposition techniques were used to prepare doped ZnO thin films such as sol gel [9, 10], magnetron sputtering [11, 12], chemical vapor deposition [13] and spray pyrolysis [14, 15]. It has been already shown that doping with rare earth element is very interesting to improve the optical properties of the ZnO host matrix [16, 17]. In the other hand doping with magnetic transition metals like Co can induce ferromagnetism at room

temperature, which is very interesting for spintronic devices [18-20]. Finally, ZnO is also an interesting candidate as transparent conducting oxide. For this purpose doping with metallic transition metal is indicated to improve its transport properties, in particular Al was shown to be the most interesting candidate [21, 22].

In this work, we report on the doping effect of aluminum on structural, electrical and optical properties of ZnO. Spray pyrolysis method was used to prepare the films because of its simplicity and mass production capability of uniform large area coatings in industrial applications.

2. Experimental

Aluminum doped ZnO (AZO) thin films were deposited on glass substrate by spray pyrolysis

technique. A homogeneous solution was prepared by dissolving zinc chloride (ZnCl_2) [0.1 M] and aluminum nitrate ($\text{Al}(\text{NO}_3)_3$) in distilled water at room temperature. Different solutions were prepared with different Al content. More details on processing doped zinc oxide were reported elsewhere [14, 23]. X'Pert Pro diffractometer was used to determine the X-Ray Diffraction (XRD) patterns with Cu $K\alpha$ 1 radiation ($\lambda = 1.54056 \text{ \AA}$). Surface morphology of AZO thin films was performed by Atomic Force Microscopy (AFM, Dimension 3100). Photoluminescence (PL) measurements were performed at room temperature in the visible range using a 355 nm line of a frequency-tripled neodymium-doped yttrium aluminum garnet-Nd-YAG-laser. The optical properties were checked by using a U-Perkin-Elmer Lambda 950 spectrophotometer. Electrical measurements were measured at room temperature using an ECOPIA Hall Effect Measurement System.

3. Results and Discussion

Fig. 1 shows the X-ray diffraction patterns of AZO thin films with different Al concentration. Both undoped and doped films have present a polycrystalline single phase and all peaks correspond to ZnO würtzite structure with a preferential orientation along the [002] direction. The lattice parameters, a and c , seem constant about 0.318 nm and 0.520 nm for a and c respectively.

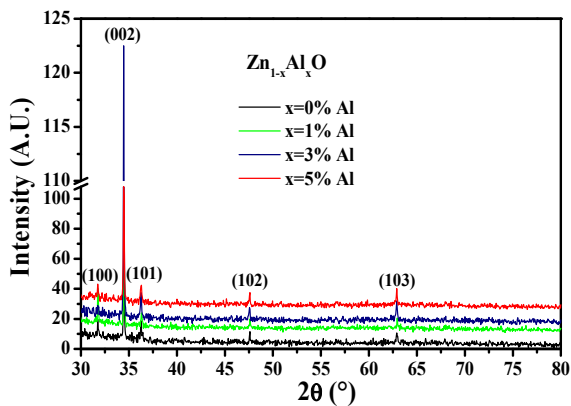


Fig. 1. XRD patterns of AZO sprayed thin films.

From the XRD results we have determined the texture coefficient (TC), which represents the texture of particular plane, whose deviation from unity implies the preferred growth. The texture factor of particular plan is defined by relation [24]:

$$TC(hkl) = \frac{I(hkl)/I_0(hkl)}{n^{-1} \sum_n I(hkl)/I_0(hkl)}, \quad (1)$$

where $I(hkl)$ is the measured relative intensity of a plane (hkl), $I_0(hkl)$ is the standard intensity of the plane (hkl) taken from JCPDS data [89-1397], n the number of diffraction peaks. The results are summarized in Table 1. One can note that all the films present a preferential orientation along the [002] direction and the higher TC value for (002) plane was observed for thin film doped with 3 % of Al. The increase in preferred orientation along (002) plane is associated to the increase in the number of grains along that plane. The average crystallites size of AZO thin films was estimated using the Scherrer's formula along the c -axis [25]:

$$D = \frac{0.9\lambda}{B \cos \theta}, \quad (2)$$

where θ is the Bragg's diffraction angle of (002) plane, B is the broadening of diffraction line at half its maximum intensity and λ the wavelength of X-rays. D values, which give the coherence length perpendicularly to the substrate, are also listed in Table 1. We can note that the higher value was obtained for 3 % Al content in agreement with the above TC values. This indicates that 3% of Al corresponds to the optimal value. Above this value, defects can be created, which can decrease both the texture and the grains size.

Table 1. Various structural parameters of AZO sprayed thin films. x : Al doping, d : thickness, D : crystallite size, TC: texture coefficient, N : number of crystallites per unit surface area, ε : strain.

x (%)	d (nm)	D (nm)	TC (002)	N ($10^{14}/\text{m}^2$)	ε (10^{-4})
0	410	67	2.30	14	5.4
1	250	57	2.26	13	4.6
3	455	94	3.01	5.4	4.6
5	455	73	2.72	12	5.0

To support the last hypothesis, we have tried to extract some information's on the evolution upon doping of dislocations in our films. Using the size of crystallites D and the thickness d , the number of crystallites N per unit volume and the strain ε are calculated using the following formula [26] and reported in Table 1:

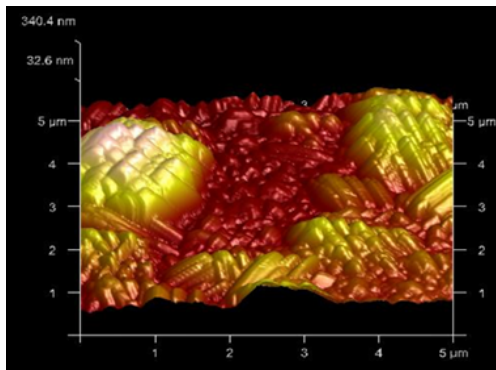
$$N = \frac{d}{D^3}, \quad (3)$$

$$\varepsilon = \frac{\Delta(2\theta) \cos \theta}{4} \quad (4)$$

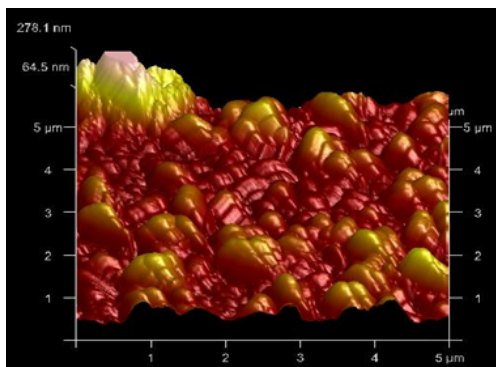
In accordance with the TC variation and d values, the small values of the strain and the dislocation density were observed for ZnO doped with 3 % of Al.

Hence, this sample presents the best crystalline quality.

Fig. 2 shows the AFM images of undoped and ZnO doped with 3 % of Al deposited on glass substrates. From the surface morphology images, it can be seen that the in-plane grain size does not change much and only a small part of the grains increased. The surface roughness of the films depends on the aluminum doping content. We observed that AZO with 3 % of Al showed a uniform grain size with the lowest root mean square (rms) value of about 24 nm, less than rms for undoped ZnO which was around 38 nm.



(a)



(b)

Fig. 2. AFM images of the surface of AZO sprayed thin films. (a) ZnO:0 % Al, (b) ZnO:3 % Al.

AZO thin films exhibit a high transmittance between 75 % and 80 % in the visible range. Absorption coefficient α has been computed and $(\alpha h\nu)^2$ versus $(h\nu)$ for undoped and AZO films is presented in Fig. 3. In the lower energy range α varies exponentially with photon energy and follows the Urbach formula [27]:

$$\alpha = \alpha_0 \exp(h\nu / E_u), \quad (5)$$

where α_0 is the constant and E_u is the Urbach energy width, which is believed to be a function of the structural disorder. The variation of $\ln\alpha$ versus photon energy for the film are displayed in the inset

of Fig. 3. The Urbach energy E_u is calculated from the slope of the linear plot. It can be seen that doping with 1 % or 3 % of Al produces an Urbach band tail width around 760 meV which is higher than the value of about 620 meV observed for undoped ZnO films, which indicate an increase of defects level in the band gap. This result seems to be contradictory with the results obtained by the structural analysis where the film with 3 % Al was shown to present the best crystalline quality. However, this cannot be directly correlated since some defects have no optical activity and therefore no influence on the obtained results.

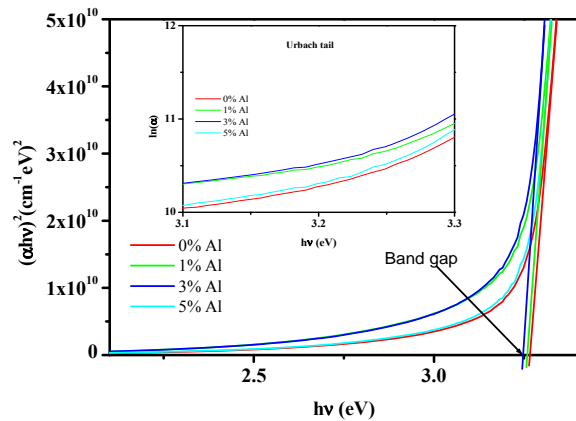


Fig. 3. $(\alpha h\nu)^2$ versus $h\nu$ and $\ln\alpha$ versus $h\nu$ of AZO sprayed thin films.

Fig. 4 shows the photoluminescence spectra at room temperature of undoped and Al-doped ZnO thin films. Lines at 355 nm and its second order at 710 nm are due to the laser source, while peak at 379 nm corresponds to the recombination of electron and hole across the gap of AZO thin films. The wide PL band centered at 510 and 697 nm characteristic of deep levels of oxygen vacancies in the ZnO matrix, and zinc or oxygen atoms in interstitial position, as it was previously reported for ZnO thin films [28]. One can note that the intensity of this wide PL band decreases at 3 % Al content, which can be attributed to the decrease of defects in this sample.

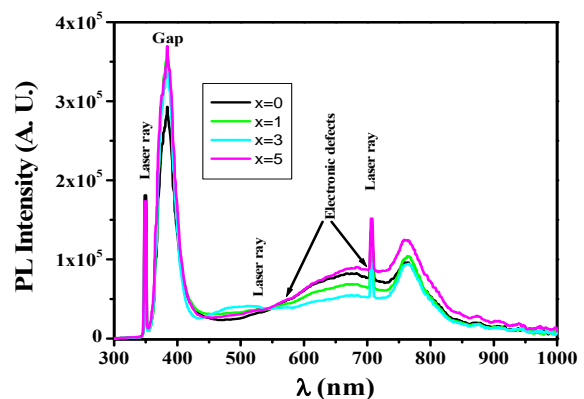


Fig. 4. Photoluminescence at room temperature of AZO sprayed thin films.

All AZO films were n-type semiconductors. The minimum of electrical resistivity was around $8.0 \cdot 10^{-2} \Omega \cdot \text{cm}^{-1}$ for 3 % Al content which is limited by the low mobility values attributed to the various carriers scattering mechanisms. In Table 2, we report ρ values obtained for AZO films prepared by various techniques.

Table 2. Comparison of electrical resistivity values of AZO thin films prepared by various techniques.

Technique	Thickness (nm)	Al (%)	ρ ($10^{-2} \Omega \cdot \text{cm}$)	Ref.
RF magnetron sputtering	450	-	0.14	[21]
Atomic layer deposition	130	2.1	0.06	[22]
Ultrasonic Spray Pyrolysis	1100-1700	3	4	[15]
Sol-gel	659	3	8000	[29]
Spray Pyrolysis	455	3	8	This work

It is interesting to note that the best electrical resistivity value obtained in this work using spray pyrolysis is comparable to the values obtained with using much more sophisticated techniques like sputtering.

4. Conclusions

Aluminum doped ZnO thin films (AZO) were deposited on glass substrates by spray pyrolysis technique. Undoped and Al-doped ZnO thin films were polycrystalline with a preferential orientation (002) along c-axis. The films were highly transparent in the visible zone. Atomic force microscopy study showed that AZO films with 3 % of Al had a uniform grain sizes with the root mean square around 24 nm. The best crystallinity and the lowest electrical resistivity were found for AZO films with 3 % of Al. These AZO films prepared by this alternative technique, can be used in various applications as in solar cells and sensor devices.

Acknowledgements

We would like to thank The Professor A. Dinia from the University of Strasbourg for photoluminescence measurements and for the constructive discussion. We also thank Dr. Khalid Nouneh from MAScIR Rabat-Morocco for his help in AFM measurements.

References


[1]. H. Gomez, A. Maldonado, M. de la L. Olvera, D. R. Acosta, Gallium-doped ZnO thin films

deposited by chemical spray, *Sol. Energy Mater. Sol. Cells*, Vol. 87, Issues 1-4, 2005, pp. 107-116.

- [2]. K. Ramamoorthy, K. Kumar, R. Chandramohan, K. Sankaranarayanan, Review on material properties of IZO thin films useful as epi-n-TCOs in opto-electronic (SIS solar cells, polymeric LEDs) devices, *Mater. Sci. Eng. B*, Vol. 126, Issue 1, 2006, pp. 1-15.
- [3]. J.-H. Oh, K.-K. Kim, T.-Y. Seong, Effects of deposition temperatures and annealing conditions on the microstructural, electrical and optical properties of polycrystalline Al-doped ZnO thin films, *Appl. Surf. Sci.*, Vol. 257, Issue 7, 2011, pp. 2731-2736.
- [4]. D. R. Sahu, S.-Y. Lin, J.-L. Huang, Improved properties of Al-doped ZnO film by electron beam evaporation technique, *Microelectron. J.*, Vol. 38, Issue 2, 2007, pp. 245-250.
- [5]. Y. Belghazi, D. Stoeffler, G. Schmerber, C. Ulhaq-Bouillet, J. L. Rehspringer, S. Colis, A. Dinia, A. Berrada, H. Aubriet, J. Petersen, C. Becker, D. Ruch, Magnetic properties of Al-doped Zn_{0.95}Co_{0.05}O films: Experiment and theory, *J. Appl. Phys.*, Vol. 105, 2009, pp. 113904.
- [6]. D. P. Norton, Y. W. Heo, M. P. Ivill, K. Ip, S. J. Pearton, M. F. Chisholm, T. Steiner, ZnO: growth, doping & processing, *Mater. Today*, Vol. 7, Issue 6, 2004, pp. 34-40.
- [7]. P. Rai, Y.-S. Kim, H.-M Song, M.-K. Song, Y.-T. Yu, The role of gold catalyst on the sensing behavior of ZnO nanorods for CO and NO₂ gases, *Sensors and Actuators B: Chemical*, Vol. 165, Issue 1, 2012, pp. 133-142.
- [8]. Y. Zeng, L. Qiao, Y. Bing, M. Wen, B. Zou, W. Zheng, T. Zhang, G. Zou, Development of microstructure CO sensor based on hierarchically porous ZnO nanosheet thin films, *Sensors and Actuators B: Chemical*, Vol. 173, 2012, pp. 897-902.
- [9]. M. Wang, K. E. Lee, S. H. Hahn, E. J. Kim, S. Kim, J. S. Chung, E. W. Shin, C. Park, Optical and photoluminescent properties of sol-gel Al-doped ZnO thin films, *Mater. Lett.*, Vol. 61, Issues 4-5, 2007, pp. 1118-1121.
- [10]. Y. Belghazi, G. Schmerber, S. Colis, J. L. Rehspringer, A. Berrada, A. Dinia, Room-temperature ferromagnetism in Co-doped ZnO thin films prepared by sol-gel method, *J. of Magn. Magn. Mater.*, Vol. 310, Issue 2, 2007, pp. 2092-2094.
- [11]. Y. H. Kim, K. S. Lee, T. S. Lee, B. Cheong, T.-Y. Seong, W. M. Kim, Effects of substrate temperature and Zn addition on the properties of Al-doped ZnO films prepared by magnetron sputtering, *Appl. Surf. Sci.*, Vol. 255, Issue 16, 2009, pp. 7251-7256.
- [12]. H. Ndilimabaka, S. Colis, G. Schmerber, D. Muller, J. J. Grob, L. Gravier, C. Jan, E. Beaurepaire, A. Dinia, *Chemical Physics Letters*, Vol. 421, Issue 1-3, 2006, pp. 184-188.
- [13]. D. Kim, I. Yun, H. Kim, Fabrication of rough Al doped ZnO films deposited by low pressure chemical vapor deposition for high efficiency thin film solar cells, *Current Applied Physics*, Vol. 10, Issue 3, 2010, pp. S459-S462.
- [14]. A. Douayar, R. Diaz, F. Cherkaoui El Moursli, G. Schmerber, A. Dinia, and M. Abd-Lefdil, Fluorine-doped ZnO thin films deposited by spray pyrolysis technique, *Eur. Phys. J. Appl. Phys.*, Vol. 53, Issue 2, 2011, pp. 20501-p4.
- [15]. A. Crossay, S. Buecheler, L. Kranz, J. Perrenoud, C. M. Fella, Y. E. Romanyuk and A. N. Tiwari,

- Spray-deposited Al-doped ZnO transparent contacts for CdTe solar cells, *Solar Energy Materials and Solar Cells*, Vol. 101, 2012, pp. 283–288.
- [16]. J. Petersen, C. Brimont, M. Gallart, G. Schmerber, P. Gilliot, C. Ulhaq-Bouillet, J. L. Rehspringer, S. Colis, C. Becker, A. Slaoui and A. Dinia, Correlation of structural properties with energy transfer of Eu-doped ZnO thin films prepared by sol-gel process and magnetron reactive sputtering, *J. Appl. Phys.*, Vol. 107, 2010, pp. 123522.
- [17]. A. Douayar, P. Prieto, G. Schmerber, K. Nouneh, R. Diaz, I. Chaki, S. Colis, A. El Fakir, N. Hassanain, A. Belayachi, Z. Sekkat, A. Slaoui, A. Dinia, M. Abd-Lefdil, Investigation of the structural, optical and electrical properties of Nd-doped ZnO thin films deposited by spray pyrolysis, *Eur. Phys. J. Appl. Phys.*, 61, 2013, 10304.
- [18]. I. Soumahoro, R. Moubah, G. Schmerber, S. Colis, M. Ait Aouaj, M. Abd-lefdil, N. Hassanain, A. Berrada, and A. Dinia, Structural, optical, and magnetic properties of Fe-doped ZnO films prepared by spray pyrolysis method, *Thin Solid Films*, Vol. 518, 2010, pp. 4593.
- [19]. Y. Belghazi, M. Ait Aouaj, M. El Yadari, G. Schmerber, C. Ulhaq-Bouillet, C. Leuvrey, S. Colis, M. Abd-lefdil, A. Berrada, and A. Dinia, Elaboration and characterization of Co-doped ZnO thin films deposited by spray pyrolysis technique, *Microelectron. J.*, Vol. 40, 2009, pp. 265-267.
- [20]. G. S. Chang, E. Z. Kurmaev, D. W. Boukhvalov, L. D. Finkelstein, A. Moewes, H. Bieber, S. Colis, and A. Dinia, Co and Al co-doping for ferromagnetism in ZnO:Co diluted magnetic semiconductors, *J. Phys. Cond. Mat.*, Vol. 21, 2009, p. 056002.
- [21]. B. L. Zhu, J. Wang, S. J. Zhu, J. Wu, D. W. Zeng and C. S. Xie, Optimization of sputtering parameters for deposition of Al-doped ZnO films by rf magnetron sputtering in Ar+H₂ ambient at room temperature, *Thin Solid Films*, Vol. 520, 2012, pp. 6963–6969.
- [22]. Y. J. Choi, S. C. Gong, D. C. Johnson, S. Gollledge, G. Y. Yeom, H. H. Park, Characteristics of the electromagnetic interference shielding effectiveness of Al-doped ZnO thin films deposited by atomic layer deposition, *Applied Surface Science*, 269, 15 March 2013, pp. 92–97.
- [23]. I. Soumahoro, G. Schmerber, A. Douayar, S. Colis, M. Abd-Lefdil, N. Hassanain, A. Berrada, D. Muller, A. Slaoui, H. Rinnert and A. Dinia, Structural, Optical, and electrical properties of Yb-doped ZnO thin films prepared by spray pyrolysis method, *J. Appl. Phys.*, Vol. 109, 2011, pp. 33708.
- [24]. S. S. Shinde, P. S. Shinde, S. M. Pawar, V. Moholkar, C. H. Bhosale, and K. Y. Rajpure, Physical properties of transparent and conducting sprayed fluorine doped zinc oxide thin films, *Solide State Sci.*, Vol. 10, Issue 9, 2008, pp.1209-1214.
- [25]. P. Scherrer, *Göttinger Nachrichten Math. Phys.*, 2, 1918, p. 98.
- [26]. S. Prabakar, M. Dhanam, CdS thin films from two different chemical baths-structural and optical analysis *J. Crystal Growth*, Vol. 285, Issues 1-2, 2005, pp. 41-48.
- [27]. J. I. Pankove, *Optical Processes in Semiconductors*, Prentice-Hall Inc., Englewood Cliffs, NJ, 1971.
- [28]. J. Petersen, C. Brimont, M. Gallart, O. Crégut, G. Schmerber, P. Gilliot, B. Hönerlage, C. Ulhaq-Bouillet, J. L. Rehspringer, C. Leuvrey, S. Colis, A. Slaoui, and A. Dinia, Optical properties of ZnO thin films prepared by sol-gel process, *Microelectron. J.*, Vol. 40, 2009, pp. 239-241.
- [29]. J. Li, J. Xu, Q. Xu, G. Fang, Preparation and characterization of Al doped ZnO thin films by sol-gel process, *Journal of Alloys and Compounds*, Vol. 542, 2012, pp. 151–156.

2014 Copyright ©, International Frequency Sensor Association (IFSA). All rights reserved.
(<http://www.sensorsportal.com>)



Universal Frequency-to-Digital Converter (UFDC-1)

- 16 measuring modes: frequency, period, its difference and ratio, duty-cycle, duty-off factor, time interval, pulse width and space, phase shift, events counting, rotation speed
- 2 channels
- Programmable accuracy up to 0.001 %
- Wide frequency range: 0.05 Hz ... 7.5 MHz (120 MHz with prescaling)
- Non-redundant conversion time
- RS-232, SPI and I²C interfaces
- Operating temperature range -40 °C... +85 °C

www.sensorsportal.com info@sensorsportal.com SWP, Inc., Canada